Magnetic susceptibility characterisation of superparamagnetic microspheres

David Tim Grob, Naomi Wise, Olayinka Oduwole, Steve Sheard

Department of Engineering Science, University of Oxford, Parks Road, Oxford OX1 3PJ, United Kingdom

Abstract

The separation of magnetic materials in microsystems using magnetophoresis has increased in popularity. The wide variety and availability of magnetic beads has fuelled this drive. It is important to know the magnetic characteristics of the microspheres in order to accurately use them in separation processes integrated on a lab-on-a-chip device.

To investigate the magnetic susceptibility of magnetic microspheres, the magnetic responsiveness of three types of Dynabeads microspheres were tested using two different approaches. The magnetophoretic mobility of individual microspheres is studied using a particle tracking system and the magnetization of each type of Dynabeads microsphere is measured using SQUID relaxometry. The magnetic beads' susceptibility is obtained at four different applied magnetic fields in the range of $38 - 70$ mT for both the mobility and SQUID measurements. The susceptibility values in both approaches show a consistent magnetic field dependence.

Keywords: Magnetic separation, Magnetic beads, Magnetic microspheres, Magnetophoresis, Magnetophoretic mobility, Susceptibility, SQUID

1. Introduction

Magnetic separation in microfluidic systems has gained a lot of attention in recent years due to its promising applications for biomarker detection in

Email addresses: tim.grob@eng.ox.ac.uk (David Tim Grob), naomi.wise@eng.ox.ac.uk (Naomi Wise), olayinka.oduwole@eng.ox.ac.uk (Olayinka Oduwole), steve.sheard@eng.ox.ac.uk (Steve Sheard)

microfluidic immunoassays. By binding magnetic beads (MBs) to specific biomarkers, the biological material inherits the magnetic properties of the magnetic bead (MB) and thus can be separated from the surrounding environment with an external magnetic field. This separation technique, based on magnetophoresis, has been applied in various applications to separate and isolate cells [1, 2, 3, 4], viruses [5, 6], proteins [7, 8] and DNA [9, 10].

MBs have diverse applications in biomedical analysis. With their small size, high surface to volume ratio, low cost and ease of functionalization with biomolecules (e.g. antibodies), MBs have shown to be a very versatile and promising tool in biomedical analysis [11, 12, 13, 14].

The MBs gain their magnetic properties by encapsulating nanoparticles of a magnetic compound, such as iron oxide, within a spherical carrier matrix (e.g. polymer). If the incorporated iron oxide particles have a size in the order of nanometres, one can observe superparamagnetism; MBs become instantly magnetized when a magnetic field is applied, but lose their magnetic moment in response to thermal fluctuation as soon as the magnetic field is removed [15, 16]. The superparamagnetic nature of MBs is an important attribute when used in cell separation. For instance, MBs can be freely distributed throughout a sample to enable interaction with the biological matter and in a second step easily collected and separated from the sample by introduction of an external magnetic field [17, 18, 19].

MBs can be made in a variety of diameters and of different materials depending on the application. A number of different MB types from various manufacturers are commercially available. However, their different manufacturing process as well as the variability in these processes make the MBs vary significantly with respect to their material properties (e.g. size distribution, iron content). Such uncertainty in the performance of MBs will hinder the development of next generation lab-on-a-chip (LOC) devices exploiting the unique characteristics of magnetophoresis for ultimate sensitivity and specificity.

The contribution made in this study addresses the fundamental issue of the suitability of MBs for the next generation of LOC devices, and in particular performance limitations attributed to the variability of MB magnetic properties. Continuous magnetic separation (also known as free-flow magnetophoresis) is a promising technique that is well suited to LOC devices for detection of disease biomarkers. In order to design LOC devices based on continuous separation of antibody-conjugated MBs with high collection efficiency, discrimination and through-put it is essential to know the mag-

netic responsiveness of the magnetic microspheres; this is especially true for devices targeting multiple biomarkers and a mixture of captured cells and proteins [20]. The magnetic responsiveness, which can be determined by measuring the MBs magnetic susceptibility [21, 22, 23], is a function of the local magnetic field. Therefore, knowing the susceptibility of the MBs at various magnetic field strengths is of great benefit for future magnetic separation devices in order to optimise their design.

One of the most widely used MBs in magnetic bio-separation to separate and immobilize proteins [24, 25], RNA complexes [26] or viruses [27] are Dynabeads magnetic microspheres. In this study, the magnetic susceptibility of three different Dynabeads MB types (MyOne, M280 and M270) is measured using a tracking system as previously reported in [28]. Additionally, the magnetic susceptibilities are verified using a superconducting quantum interference device (SQUID).

In order to study the magnetic field dependence of the MBs, their magnetic susceptibility is determined at four different magnetic field magnitudes, ranging between 38 mT and 70 mT, in both measurement methods. Either method gives a volume averaged susceptibility value at a given externally applied magnetic field, which can be used in magnetic separation research to predict the separation efficiency and magnetic microsphere trajectories.

2. Theoretical model

The trajectory of a single MB in a liquid medium under the influence of an imposed magnetic field gradient is governed by two dominant forces, the magnetic force and the Stokes' drag. Therefore, the following equation of motion can be developed [11]:

$$m_b \frac{d\mathbf{u}_b}{dt} = \mathbf{F}_M + \mathbf{F}_D \tag{1}$$

where m_b and $\mathbf{u}_b$ are the mass and velocity of the MB, and $\mathbf{F}_M$ and $\mathbf{F}_D$ are the magnetic force and the Stokes' drag, respectively. Here, the bold letters indicate a vector.

The magnetic force, $\mathbf{F}_M$, acting on a single domain MB can generally be expressed as [29]:

$$\mathbf{F}_M = (\mathbf{m}_b(|\mathbf{B}|) \cdot \nabla)\mathbf{B} \tag{2}$$

with $\mathbf{m}_b(|\mathbf{B}|)$ the net magnetic moment of the MB for a given applied magnetic field and $\nabla|\mathbf{B}|$ the gradient of the magnetic flux density. For MBs, where the magnetic moment does not vary strongly within the characteristic dimension of the bead and by assuming that the physical properties of the bead and the suspending fluid are homogeneous and isotropic, Equation 2 can be written as [30]:

$$\mathbf{F}_M = V_b \Delta\chi \frac{\nabla \mathbf{B}^2}{2\mu_0} \tag{3}$$

where V_b is the volume of the MB, μ_0 is the magnetic permeability of free space, $\mathbf{B}$ is the magnetic flux density and $\Delta\chi = \chi_b - \chi_f$ describes the difference in magnetic susceptibility of the MB (χ_b) and the surrounding medium (χ_f). The susceptibility of the surrounding medium is often neglected because its value is at least four orders of magnitude smaller than the susceptibility of the MB [31, 32]. Thus, it is safe to neglect the effect of the magnetic properties of the suspending medium and simplify Equation 3 by only using χ_b, the magnetic susceptibility of the MB, instead of $\Delta\chi$:

$$\mathbf{F}_M = V_b \chi_b \frac{\nabla \mathbf{B}^2}{2\mu_0} \tag{4}$$

The susceptibility of the magnetic microspheres, χ_b is often assumed to be independent of the applied magnetic field [13, 21], which might be a justifiable approximation in weak magnetic fields. In this study, this approximation is not made and the microspheres' susceptibility is assumed to be dependent on the externally applied magnetic field ($\chi_b(|\mathbf{B}|)$).

The drag force, $\mathbf{F}_D$, acting upon a spherical object can be expressed as [33]:

$$\mathbf{F}_D = -6\pi\eta r \mathbf{u}_b \tag{5}$$

The parameters η, r and $\mathbf{u}_b$ are the dynamic viscosity of the suspending medium, the bead radius and the velocity of the bead, respectively.

For micron-sized beads the terminal velocity is reached in microseconds and the equation of motion (Equation 1) can be simplified; for the application considered it is sufficient to assume:

$$\mathbf{F}_M = -\mathbf{F}_D \tag{6}$$

Using Equation 4 and Equation 5 in the simplified equation of motion (Equation 6) one obtains the following equation for the magnetically induced terminal velocity:

$$\mathbf{u}_b = \underbrace{\frac{\chi_b V_b}{6\pi\eta r}}_{\nu_b} \cdot \underbrace{\frac{\nabla \mathbf{B}^2}{2\mu_0}}_{S} \tag{7}$$

This velocity, $\mathbf{u}_b$, also known as the magnetic drift velocity, is the result of a magnetic force created on the magnetic microsphere by the interaction with the imposed magnetic energy gradient. An interesting interpretation of Equation 7 is that it depends on a purely bead related term and a field related term; it is the product of magnetic microsphere and suspending viscous medium properties, and the applied magnetic field properties. The two factors of this product, in Equation 7, can be usefully defined as the magnetophoretic mobility of the MB, ν_b, and the magnetophoretic driving force, S.

3. Material and methods

3.1. Superparamagnetic microspheres

Three different types of Dynabeads were purchased in a liquid buffer suspension ($\approx\ 0.6 \times 10^8 - 1 \times 10^{10}$ microspheres/mL) from Thermo Fisher Scientific (Thermo Fisher Scientific Inc.), as listed in Table 1. All beads have a common structure incorporating iron oxides (Fe_3O_4 or γ-Fe_2O_3) in a porous host matrix; creating a surface that can be functionalized [34]. The iron oxide is in the form of a fixed dispersion of nano-sized particles within the spherical host matrix. The iron oxide particle size is typically in the range of nanometres, such that their magnetic behaviour is superparamagnetic due to their single domain state; they are uniformly and randomly distributed in the host matrix. This multi-phase structure, as well as its superparamagnetic properties, has been verified by Fonnum et al. [35].

The magnetic microspheres' diameter was independently measured by analysing scanning electron microscopy (SEM) images. All MBs are approximately spherical in shape with a highly uniform size distribution, as can be seen in Figure 1. Their monodispersity provides a consistent diameter with a tight size distribution with a coefficient of variation of less than 3%, which is below the stated range of the manufacturer (see Table 1).

Table 1: Physical characteristics of the Dynabeads' density, iron content and diameter (d_M) as stated by the manufacturer [36]. The diameter (d_m) was independently measured for comparison, by analysing scanning electron microscopy (SEM) images, see Figure 1.

Magnetic bead type	Density $[g/c\mathrm{m}^3]$	Iron content [wt. %]	Diameter	
			d_M [μm]	d_m [μm]
MyOne	1.8	26	1.05	1.05 ± 0.03
M280	1.4	12	2.8	2.79 ± 0.05
M270	1.6	14	2.8	2.75 ± 0.07

3.2. Magnetophoresis experiment

To compare the magnetophoretic responsiveness of single MBs, their drift velocities in a stationary fluid was observed, similar to the work of Häfeli et. al. [21]. In Ref [21] the MBs were kept at a constant distance from the magnet; in our study, however, the beads' velocities were measured at different distances away from a neodymium-iron boron (NdFeB) magnet ($42 \times 8 \times 10$mm) using an inverted microscope (Leitz Wetzlar, Germany) with a long working distance $20\times$ objective lens (Comar Optics, Cambridge, UK) and a CCD camera (μEye Imaging Development Software, Germany). The trajectories of single MBs moving towards the magnet were observed in a FastRead 102 microscope counting slide (Immune Systems, UK), which consists of a set of easy-to-fill fluid *observation chambers*. Each observation chamber has a counting grid etched to its surface for easy determination of viewing location, as depicted in Figure 2.

Prior to the velocity measurements, all three bead types were diluted in deionized water to a concentration of $0.9 - 1.4 \times 10^5$ particles/ml. This concentration was then confirmed by observing the number of beads on the counting grid of the observation chamber. Visual inspection of previously carried out experiments had shown that such low concentrations successfully avoid bead interactions [37]. The bead solution was placed in an ultrasonic bath for 10 minutes to break up aggregates and fully suspend the microspheres. A volume of 20 μl of each bead solution was pipetted into an observation chamber; the liquid solution is drawn into the chamber by capillary action. Once the bead solution had filled the observation chamber and the MBs were stationary, an external magnetic field was applied by accurately positioning the NdFeB magnet adjacent to the observation chamber. The permanent magnet is attached to a translation stage, which allowed accurate

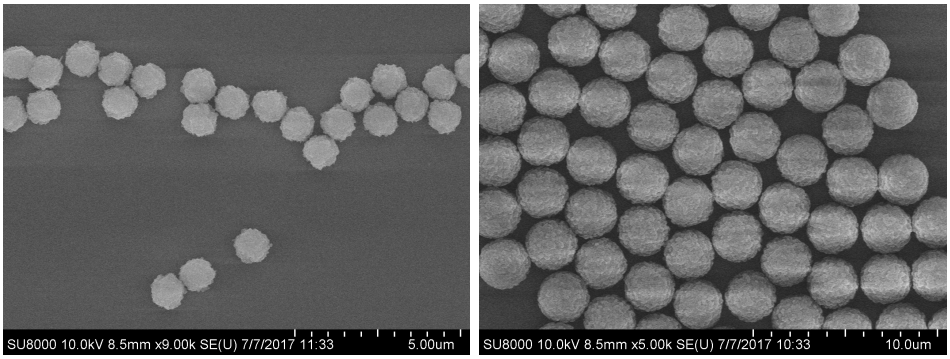

(a) MyOne (b) M280

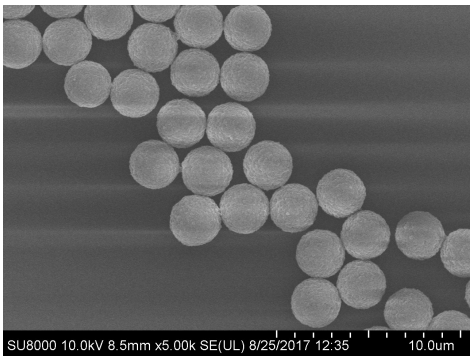

(c) M270

Figure 1: SEM images of the three magnetic bead products manufactured by Dynabeads. The images were taken using a FEI Quanta 600 SEM. The accelerating voltage was set to 10 kV.

movement of the magnet to different positions, a_b, away from the counting grid as indicated in Figure 2.

The trajectories of single MBs at different distances a_b ($a_b = [10, 12, 14, 16]$ mm) from the magnet surface were recorded and analysed off-line using the freely available software *ImageJ* with the open source particle tracking plug-in *MTrackJ*. MBs were observed moving in the x direction towards the magnet over a distance of approximately 55 μm. By measuring the time taken, the magnetically induced drift velocity, u_b, was calculated for each MB type in Table 1.

In order to obtain magnetic susceptibility, χ_b, of the MBs, the magnitude of the magnetophoretic mobility, ν_b, was first calculated by dividing the measured bead velocity, u_b, by the magnetophoretic driving force, S (see

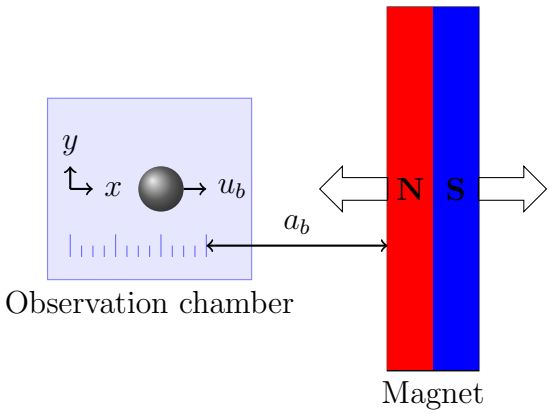

Figure 2: Schematic of the experimental setup used to determine the magnetically induced velocity of single MBs. Figure is not drawn to scale.

Equation 7). In this study, the magnetophoretic driving force at the various positions was calculated by measuring the magnetic flux density along the centre line of the bar magnet with a Hall effect probe (5100 Series Sypris Test & Measurement F.W.Bell 12/04). The measured points were fitted with an exponential curve, which was subsequently used to obtain the magnetophoretic driving force as a continuous function. The difference between the measurement and the fitted exponential curve was found to be no more than 0.6% within the area of interest, which is the region between 10 mm and 16 mm away from the magnet surface where measurements are taken. The magnetic flux density along the centre line of the bar magnet was also simulated using ANSYS Maxwell. The magnetic flux density from the ANSYS simulation and measurement is shown in Figure 3.

The measured flux density is found to reduce from 70mT to 38mT when the distance, a_b, is increased from 10mm to 16mm, and the corresponding flux gradient changed from 8.3mT/mm to 3.4mT/mm.

3.3. SQUID measurement

In order to obtain independent and consistent magnetic information for all superparamagnetic microspheres, the magnetization curve for each MB type was measured using a SQUID measurement system.

The SQUID relaxometry technique has been described in detail in other literature [38, 39]. A brief explanation is given here. The SQUID sensor measures the magnetic moment by magnetizing the sample using an applied

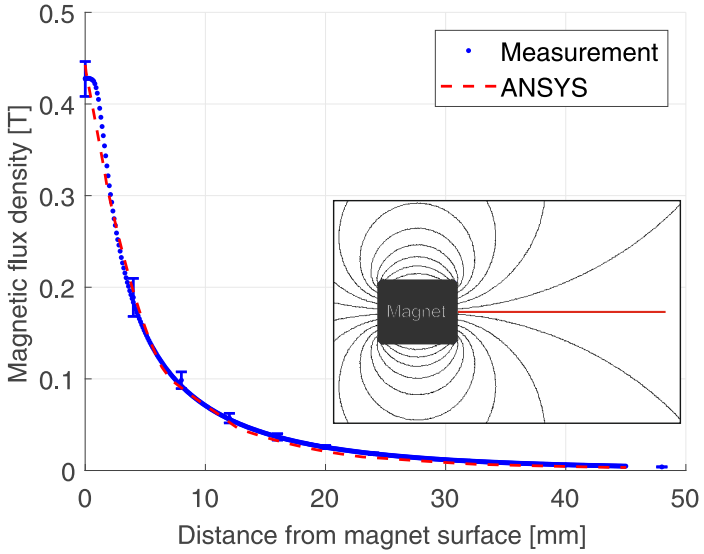

Figure 3: Characterization of the magnetic flux density of a N42 Neodymium bar magnet ($42 \times 8 \times 10$ mm). The magnetic flux density is measured along the centre line of the bar magnet as depicted in the inset, starting at the surface of the magnet to 45 mm away, with a step size of 0.1 mm. The error bars are calculated by taking the standard deviation of 14 independent magnetic field measurements at specific distances away from the magnet surface. The magnetic flux density along the same path is also simulated in ANSYS Maxwell and compared. Measurement of bead drift velocity is only taken over the range of $10 - 16$ mm away from the magnet.

magnetic field pulse capable of providing a range from -5 T to 5 T with a frequency of $0.5 - 4$ Hz.

To measure the magnetic response of the different Dynabeads, a measurement sample from the same manufacturer's batch as the one used in the magnetophoresis experiment (Section 3.2) was prepared for each MB type. The samples were made by drying a small amount of each bead solution in an oven at 65°C. The dry MB *powder* was put in a sample holder. The sample holder was sealed to ensure a fixed sample position and attached to a SQUID probe. The probe was lowered into the SQUID measurement system (Quantum Design Magnetic Property Measurement System MPMS-XL) where a magnetic field was applied at a temperature of 300 K.

Hysteresis loops were used to determine the susceptibility of the MB types by taking the ratio of the sample magnetization and the applied magnetic flux density. The susceptibility of the MB sample was individually calculated at

four different magnetic fields over the range of $38 - 70$ mT, corresponding to the magnetic flux densities at the four magnet positions ($a_b = [10, 12, 14, 16]$ mm) used in the magnetophoresis experiment described above.

4. Results

4.1. Magnetophoresis results

Figure 4 shows the magnetically induced drift velocity (Figure 4a) and the derived magnetophoretic mobility (Figure 4b) of the three observed bead types for the different distances a_b away from the magnet.

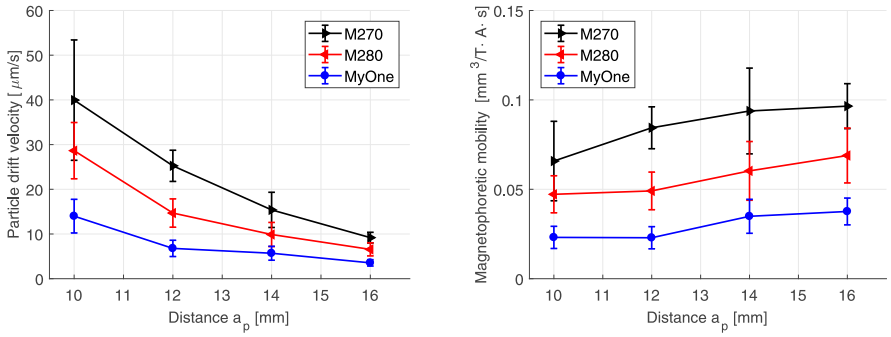

(a) (b)

Figure 4: Results of the magnetophoresis study, where (a) shows the measured magnetic drift velocity at various distances away from the magnet and (b) the corresponding calculated magnetophoretic mobility of the three analysed Dynabeads MB types.

The drift velocity and the magnetic mobility of the MBs appear to be negatively correlated, with the mobility dependent on the distance from the magnet ($10 - 16$ mm). This implies that the mobility is a function of the externally applied magnetic field.

Based on the measured mobilities and MB diameters d_m (Table 1), the susceptibility of the MBs can be calculated. Table 2 lists the different susceptibilities at four different magnetic fields, which correspond to the four magnet positions, a_b, used in Figure 4b.

The different magnetic susceptibility values for the various bead types confirms that the structure of the MBs influences their magnetic responsiveness. The increase in susceptibility, when decreasing the applied magnetic field, which is equivalent to increasing distance from the magnet, is attributed to the non-linearity of the susceptibility.

Table 2: Averaged susceptibility of the three types of Dynabeads calculated at four different magnetic flux density, which correspond to the four distances, a_b, away from the magnet. The magnetic flux density values 70 mT, 56 mT, 46 mT, and 38 mT correspond to the distances $a_b = 10$ mm, $a_b = 12$ mm, $a_b = 14$ mm, $a_b = 16$ mm, respectively. The susceptibilities are calculated based on the measured magnetically induced velocities of single MBs. At each magnetic field magnitude the obtained susceptibilities are averaged and one standard deviation is given. The total number of observations for each bead type was 46, 248 and 92 for MyOne, M280 and M270, respectively.

Particle type	χ_p			
	70 mT	56 mT	46 mT	38 mT
MyOne	0.34±0.09	0.33±0.08	0.54±0.14	0.58±0.10
M280	0.11±0.02	0.11±0.02	0.13±0.02	0.15±0.03
M270	0.14±0.04	0.19±0.03	0.21±0.06	0.22±0.02

4.2. SQUID results

Figure 5 shows the measured hysteresis loops of the three different types of Dynabeads. The hysteresis loops give the magnetization of the MB types at a specific applied magnetic field and incorporate all magnetic properties (e.g. remanence) of the MB sample.

From these curves (Figure 5) the remanence, M_R and magnetic susceptibility of the particle sample, χ, are estimated. In the magnetization study the subscript b in the susceptibility parameter χ is dropped, because the SQUID measurement is not done on individual beads but on a sample containing a large number of beads.

The remanence was observed to be no more than 84 A/m (Figure 5b), which is a value consistent with the literature; refer to Shevkoplyas et. al. [30] or Hien et. al. [40]. Magnetic remanence is due to thermally blocked magnetic moments of the incorporated iron oxide nano-sized particles [35]. Many research papers on magnetic separation discard the remanence of the MBs, because its value is assumed to be significantly smaller than the applied magnetic field. However, not taking remanence into account may compromise the susceptibility parameter as concluded by Shevkoplyas et. al. [30]. Using all data points along the hysteresis loop to determine the susceptibility as a function of the applied magnetic field takes all magnetic parameters and conditions into account, including remanence.

The susceptibility is measured at the four magnetic field magnitudes cor-

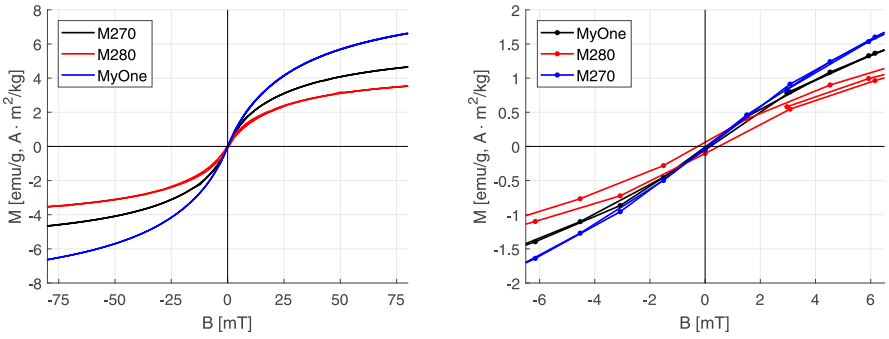

(a) (b)

Figure 5: Magnetization curves of the three different types of Dynabeads when a magnetic field is applied in the range of (a) ±75 mT and (b) ±6 mT. The magnetization of the MB types saturate in fields stronger than ≈ 0.5 T (not shown) with a saturation magnetization of 9.4 Am^2/kg, 6.4 Am^2/kg and 4.6 Am^2/kg for MyOne, M270 and M280 Dynabeads microspheres, respectively. The curves were measured with a Quantum Design MPMS-XL SQUID magnetometer at room temperature (300 K).

responding to the data reported in Section 4.1. The susceptibilities at the various magnetic flux densities at the different distances, a_b, away from the magnet surface are listed in Table 3; the SQUID measured susceptibilities also show a monotonic increase.

Table 3: Susceptibility values of the analysed MB types measured with a SQUID system (Quantum Design Magnetic Property Measurement System MPMS-XL). The susceptibilities are measured at four applied magnetic fields, ranging from 38 − 70 mT.

Particle type	χ			
	70 mT	56 mT	46 mT	38 mT
MyOne	0.22	0.26	0.30	0.34
M280	0.09	0.11	0.13	0.15
M270	0.14	0.16	0.19	0.22

5. Discussion

A clear difference in magnetophoretic mobility can be seen between the three analysed MB types (see Figure 4b). The M270 beads have the largest

magnetophoretic mobility, followed by the M280 and MyOne beads. The different magnetophoretic mobilities for the different MB types come from their different size and iron content (see Table 1). Even though the MyOne beads have the highest density of iron they exhibit the smallest magnetophoretic mobility due to their small volume.

The magnetic mobility of three types of Dynabeads was measured in this study. The variation in mobility within one type of bead at the applied magnetic fields cannot be attributed to variation in bead diameter alone because the measured size distribution is found to be numerically insignificant in comparison. This conclusion is in contrast to the findings of Xu et al. where the spread of the different magnetically induced velocities are predominaltely attibuted to the bead size distribution [41]. The statistical variation in iron content between single MBs, is not known by the authors and might differ between different manufactured batches [42]. Due to the complex structure of the MBs it is unlikely that every bead will exhibit the exact same magnetic responsiveness. Thus, the observed variation in magnetic mobility reported in this study is attributed to varying iron content.

The susceptibility for the analysed MB types of the two measurement methods, magnetophoresis study and SQUID measurements, show similar trends with decreasing applied magnetic field. The determined susceptibility values also show a good agreement with values stated by the manufacturer and in the literature [28, 35, 43, 44, 45, 46, 47]. In the literature the susceptibility ranges between 0.26 and 1.4 for MyOne beads [35, 44], between 0.14 and 0.76 for M280 beads [35, 45, 47] and a value of ≈ 0.17 [44, 46] for the M270 beads. The susceptibility values in this study are within the range of values previously published in the literature.

The monotonic increase of susceptibility with decreasing magnetic field can be seen across all particle types and in both measurement methods (magnetophoresis study and SQUID measurements) and is a consequence of a magnetic field dependent magnetization of the MBs (Equation 2). The magnetization curves in Figure 5 reveal that the linear relationship $\mathbf{M} = \chi\mathbf{H}$ between magnetization and applied field is a simplification and might only be a valid approximation for magnetic fields $|\mathbf{B}| \leq 6$ mT, based on the observations in Figure 5b. In addition, the remanence of the MBs may contribute to the behaviour of the beads at even lower magnetic fields and should not be neglected as discussed by Shevkoplyas et. al. [30]. At larger magnetic fields, the data presented in Figure 5a should be considered to account for the non-linear behaviour of the susceptibility. Many publications in the lit-

erature [48], however, neglect remanence and the magnetic field dependence of the susceptibility, leading to modelling errors.

6. Conclusion

The magnetic responsiveness of three different types of Dynabeads were tested using two different approaches. The magnetophoretic mobility of single MBs was studied using a particle tracking system and the magnetization of the same beads measured using SQUID relaxometry.

The magnetophoretic mobility of individual beads is measured over a range of $38-70$ mT using a permanent magnet. The monotonic reduction in mobility of the MBs as they approach the permanent magnet is attributed to a reduction in susceptibility with magnetic field strength. The same negative correlation between the magnitude of the magnetic field and the susceptibility of the magnetic microspheres was observed by analysing hysteresis curves of MB samples, obtained from SQUID measurements. The change in mobility results from the non-linearity of the magnetic susceptibility with respect to the applied magnetic field. In cases where the trajectory of a MBs needs to be determined accurately, the observations in this study conclude that a constant susceptibility does not lead to accurate calculations and instead the non-linear behaviour of the susceptibility should be taken into account. A constant susceptibility can only be assumed when the MBs interact over a narrow magnetic field regime, but the susceptibility value should still account for the magnitude of the applied magnetic field.

The consistent values of the susceptibility obtained by the magnetophoresis analysis compared to those from the SQUID measurement suggest that particle tracking is a viable technique for determination of susceptibility of superparamagnetic microspheres over a range of magnetic flux densities. Unlike average magnetic susceptibility data obtained from SQUID or VSM (Vibrating Sample Magnetometer), the particle tracking system can characterize the magnetic properties of single MBs.

The comparison of the three types of Dynabeads also highlights the differences of their physical properties and made it evident that some MB types are potentially more suitable for lab-on-a-chip magnetic cell separation than others. A high magnetic mobility with a narrow distribution is desirable because separation time and reproducibility are often limiting factors, especially for continuous magnetic separation where the interaction of the MBs with the magnet is time critical. Thus, a high magnetophoretic mobility ensures that

even at short interaction time the MBs separate. A narrow magnetophoretic mobility distribution allows for accurate MB trajectory predictions and will enhance separation efficiency. Dynabeads M270 magnetic microspheres meet the above criteria and are therefore the best choice for magnetic particle separation based on this study. The magnetophoretic mobilities and susceptibility values found in this paper will help scientists to predict the motion of beads more accurately.

Acknowledgements

This work would not have been possible without the financial support of the Janggen-Poehn-Stiftung from St. Gallen in Switzerland. Special thank also goes to Phil Wiseman from the Chemistry Department at Oxford University for use of the SQUID measurement equipment.

[1] J. P. Hancock, J. T. Kemshead, A rapid and highly selective approach to cell separations using an immunomagnetic colloid, Journal of immunological methods 164 (1) (1993) 51–60.

[2] K. E. McCloskey, J. J. Chalmers, M. Zborowski, Magnetic cell separation: characterization of magnetophoretic mobility, Analytical chemistry 75 (24) (2003) 6868–6874.

[3] N. Xia, T. P. Hunt, B. T. Mayers, E. Alsberg, G. M. Whitesides, R. M. Westervelt, D. E. Ingber, Combined microfluidic-micromagnetic separation of living cells in continuous flow, Biomedical microdevices 8 (4) (2006) 299–308.

[4] M. Zborowski, J. J. Chalmers, Magnetic cell separation, Vol. 32, Elsevier, 2011.

[5] K.-H. Heermann, Y. Hagos, R. Thomssen, Liquid-phase hybridization and capture of hepatitis b virus dna with magnetic beads and fluorescence detection of pcr product, Journal of virological methods 50 (1) (1994) 43–57.

[6] J. Pipper, M. Inoue, L. F. P. Ng, P. Neuzil, Y. Zhang, L. Novak, Catching bird flu in a droplet, Nature medicine 13 (10) (2007) 1259.

[7] S.-K. Kim, L. Devine, M. Angevine, R. DeMars, P. B. Kavathas, Direct detection and magnetic isolation of chlamydia trachomatis major outer membrane protein-specific cd8+ ctls with hla class i tetramers, The Journal of Immunology 165 (12) (2000) 7285–7292.

[8] R. De Palma, G. Reekmans, C. Liu, R. Wirix-Speetjens, W. Laureyn, O. Nilsson, L. Lagae, Magnetic bead sensing platform for the detection of proteins, Analytical chemistry 79 (22) (2007) 8669–8677.

[9] J. Vuosku, L. Jaakola, S. Jokipii, K. Karppinen, T. Kmrinen, V.-P. Pelkonen, A. Jokela, T. Sarjala, A. Hohtola, H. Hggman, Does extraction of dna and rna by magnetic fishing work for diverse plant species?, Molecular biotechnology 27 (3) (2004) 209–215.

[10] S. W. Yeung, I.-M. Hsing, Manipulation and extraction of genomic dna from cell lysate by functionalized magnetic particles for lab on a chip applications, Biosensors and Bioelectronics 21 (7) (2006) 989–997.

[11] Q. A. Pankhurst, J. Connolly, S. Jones, J. Dobson, Applications of magnetic nanoparticles in biomedicine, Journal of physics D: Applied physics 36 (13) (2003) R167–.

[12] M. A. Gijs, Magnetic bead handling on-chip: new opportunities for analytical applications, Microfluidics and Nanofluidics 1 (1) (2004) 22–40.

[13] N. Pamme, Magnetism and microfluidics, Lab Chip 6 (1) (2006) 24–38.

[14] C. Bárcena, A. K. Sra, J. Gao, Applications of magnetic nanoparticles in biomedicine, in: Nanoscale magnetic materials and applications, Springer, 2009, pp. 591–626.

[15] W. F. Brown, Thermal fluctuations of a single-domain particle, Phys. Rev. 130 (5) (1963) 1677–1686.

[16] D. C. Jiles, Introduction to magnetism and magnetic materials, CRC press, 1998.

[17] X. Xiao, X. Yang, T. Liu, Z. Chen, L. Chen, H. Li, L. Deng, Preparing a highly specific inert immunomolecular-magnetic beads for rapid detection and separation of s. aureus and group g streptococcus, Applied microbiology and biotechnology 75 (5) (2007) 1209–1216.

[18] S.-I. Tu, S. Reed, A. Gehring, Y. He, G. Paoli, Capture of escherichia coli o157: H7 using immunomagnetic beads of different size and antibody conjugating chemistry, Sensors 9 (2) (2009) 717–730.

[19] R. Mendes, S. Laschi, D. Stach-Machado, L. Kubota, G. Marrazza, A disposable voltammetric immunosensor based on magnetic beads for early diagnosis of soybean rust, Sensors and Actuators B: Chemical 166 (2012) 135–140.

[20] W. Huang, C.-L. Chang, N. D. Brault, O. Gur, Z. Wang, S. I. Jalal, P. S. Low, T. L. Ratliff, R. Pili, C. A. Savran, Separation and dual detection of prostate cancer cells and protein biomarkers using a microchip device, Lab on a Chip 17 (3) (2017) 415–428.

[21] U. O. Häfeli, M. A. Lobedann, J. Steingroewer, L. R. Moore, J. Riffle, Optical method for measurement of magnetophoretic mobility of individual magnetic microspheres in defined magnetic field, Journal of magnetism and magnetic materials 293 (1) (2005) 224–239.

[22] A. Ivanov, A. Pshenichnikov, Magnetophoresis and diffusion of colloidal particles in a thin layer of magnetic fluids, Journal of Magnetism and Magnetic Materials 322 (17) (2010) 2575–2580.

[23] A. F. Pshenichnikov, A. S. Ivanov, Magnetophoresis of particles and aggregates in concentrated magnetic fluids, Phys. Rev. E 86 (5) (2012) 051401–.

[24] M. Kobayashi, M. Aida, H. Nagaoka, N. A. Begum, Y. Kitawaki, M. Nakata, A. Stanlie, T. Doi, L. Kato, I.-m. Okazaki, Aid-induced decrease in topoisomerase 1 induces dna structural alteration and dna cleavage for class switch recombination, Proceedings of the National Academy of Sciences 106 (52) (2009) 22375–22380.

[25] A. Säll, K. Sjöholm, S. Waldemarson, L. Happonen, C. Karlsson, H. Persson, J. Malmström, Development of phage-based antibody fragment reagents for affinity enrichment of bacterial immunoglobulin g binding proteins, Journal of proteome research 14 (11) (2015) 4704–4713.

[26] B. R. So, L. Wan, Z. Zhang, P. Li, E. Babiash, J. Duan, I. Younis, G. Dreyfuss, A u1 snrnp-specific assembly pathway reveals the smn complex as a versatile hub for rnp exchange, Nature structural & molecular biology 23 (3) (2016) 225–230.

[27] T. R. Clinton, M. T. Weinstock, M. T. Jacobsen, N. Szabo-Fresnais, M. J. Pandya, F. G. Whitby, A. S. Herbert, L. I. Prugar, R. McKinnon, C. P. Hill, Design and characterization of ebolavirus gp prehairpin intermediate mimics as drug targets, Protein Science 24 (4) (2015) 446–463.

[28] N. Wise, T. Grob, K. Morten, I. Thompson, S. Sheard, Magnetophoretic velocities of superparamagnetic particles, agglomerates and complexes, Journal of Magnetism and Magnetic Materials 384 (2015) 328–334.

[29] L. D. Landau, J. S. Bell, M. J. Kearsley, L. P. Pitaevskii, E. M. Lifshitz, J. B. Sykes, Electrodynamics of continuous media, Vol. 8, elsevier, 2013.

[30] S. S. Shevkoplyas, A. C. Siegel, R. M. Westervelt, M. G. Prentiss, G. M. Whitesides, The force acting on a superparamagnetic bead due to an applied magnetic field, Lab on a chip 7 (10) (2007) 1294–1302.

[31] A. Winkleman, K. L. Gudiksen, D. Ryan, G. M. Whitesides, D. Greenfield, M. Prentiss, A magnetic trap for living cells suspended in a paramagnetic buffer, Appl. Phys. Lett. 85 (12) (2004) 2411–2413.

[32] W. M. Haynes, CRC Handbook of Chemistry and Physics, 97th Edition, CRC Press, 2016.

[33] J. Happel, H. Brenner, Low Reynolds number hydrodynamics: with special applications to particulate media, Vol. 1, Springer Science & Business Media, 2012.

[34] S. Davis, Microspheres and drug therapy: pharmaceutical, immunological, and medical aspects, Elsevier, 1984.

[35] G. Fonnum, C. Johansson, A. Molteberg, S. Møup, S.up, E. Aksnes, Characterisation of dynabeads by magnetization measurements and mössbauer spectroscopy, Journal of Magnetism and Magnetic Materials 293 (1) (2005) 41–47.

[36] T. Scientific, Dynabeads magnetic separation technology (11 2015).
URL http://www.thermofisher.com/uk/en/home/brands/product-brand/dynal.html?ci

[37] O. Oduwole, D. T. Grob, S. Sheard, Comparison between simulation and experimentally observed interactions between two magnetic beads in a fluidic system, Journal of Magnetism and Magnetic Materials 407 (2016) 8–12.

[38] E. Flynn, H. Bryant, A biomagnetic system for in vivo cancer imaging, Physics in medicine and biology 50 (6) (2005) 1273–.

[39] N. L. Adolphi, D. L. Huber, J. E. Jaetao, H. C. Bryant, D. M. Lovato, D. L. Fegan, E. L. Venturini, T. C. Monson, T. E. Tessier, H. J. Hathaway, Characterization of magnetite nanoparticles for squid-relaxometry and magnetic needle biopsy, Journal of magnetism and magnetic materials 321 (10) (2009) 1459–1464.

[40] L. T. Hien, L. K. Quynh, V. T. Huyen, B. D. Tu, N. T. Hien, D. M. Phuong, P. H. Nhung, D. T. H. Giang, N. H. Duc, Dna-magnetic bead detection using disposable cards and the anisotropic magnetoresistive sensor, Advances in Natural Sciences: Nanoscience and Nanotechnology 7 (4) (2016) 045006.

[41] J. Xu, K. Mahajan, W. Xue, J. O. Winter, M. Zborowski, J. J. Chalmers, Simultaneous, single particle, magnetization and size measurements of micron sized, magnetic particles, Journal of Magnetism and Magnetic Materials 324 (24) (2012) 4189–4199.

[42] K. van Ommering, J. H. Nieuwenhuis, L. J. van IJzendoorn, B. Koopmans, M. W. J. Prins, Confined brownian motion of individual magnetic nanoparticles on a chip: Characterization of magnetic susceptibility, Applied physics letters 89 (14) (2006) 142511.

[43] M. Zborowski, L. R. Moore, P. S. Williams, J. J. Chalmers, Separations based on magnetophoretic mobility, Separation science and technology 37 (16) (2002) 3611–3633.

[44] M. D. Tarn, S. A. Peyman, D. Robert, A. Iles, C. Wilhelm, N. Pamme, The importance of particle type selection and temperature control for on-chip free-flow magnetophoresis, Journal of Magnetism and Magnetic Materials 321 (24) (2009) 4115–4122.

[45] B. Sinha, S. Anandakumar, S. Oh, C. Kim, Micro-magnetometry for susceptibility measurement of superparamagnetic single bead, Sensors and Actuators A: Physical 182 (2012) 34–40.

[46] P. Li, D. Kilinc, Y.-F. Ran, G. U. Lee, Flow enhanced non-linear magnetophoretic separation of beads based on magnetic susceptibility, Lab on a Chip 13 (22) (2013) 4400–4408.

[47] H. Lee, D. Ham, R. M. Westervelt, CMOS biotechnology, Springer, 2007.

[48] N. Pamme, A. Manz, On-chip free-flow magnetophoresis: continuous flow separation of magnetic particles and agglomerates, Analytical chemistry 76 (24) (2004) 7250–7256.